VISUAL-GRAVITOINERTIAL INTERACTIONS FOR ALTITUDE PERCEPTION DURING MANUAL AND SUPERVISORY CONTROL

Martine Godfroy-Cooper, Jean-Christophe Sarrazin, E Bachelder, J Miller, François Denquin, Benoit Bardy

▶ **To cite this version:**

Martine Godfroy-Cooper, Jean-Christophe Sarrazin, E Bachelder, J Miller, François Denquin, et al.. VISUAL-GRAVITOINERTIAL INTERACTIONS FOR ALTITUDE PERCEPTION DURING MANUAL AND SUPERVISORY CONTROL. 77th Annual Forum & Technology Display, May 2021, VIRTUEL, United States. hal-03602529

HAL Id: hal-03602529
https://hal.science/hal-03602529

Submitted on 9 Mar 2022

HAL is a multi-disciplinary open access archive for the deposit and dissemination of scientific research documents, whether they are published or not. The documents may come from teaching and research institutions in France or abroad, or from public or private research centers.

L'archive ouverte pluridisciplinaire **HAL**, est destinée au dépôt et à la diffusion de documents scientifiques de niveau recherche, publiés ou non, émanant des établissements d'enseignement et de recherche français ou étrangers, des laboratoires publics ou privés.

VISUAL-GRAVITOINERTIAL INTERACTIONS FOR ALTITUDE PERCEPTION DURING MANUAL AND SUPERVISORY CONTROL

Dr. M. Godfroy-Cooper
Research Psychologist
SJSU /U.S. Army
TDD AvMC
Moffett Field, California, USA

Dr. J.C. Sarrazin
Research Scientist
ICNA/DTIS/ONERA
Salon de Provence, France

Dr. E. Bachelder
Research Engineer
SJSURF/U.S. Army
TDD AvMC
Moffett Field, 94035 CA

J. D. Miller
Research Engineer
SJSU/U.S. Army
TDD AvMC
Moffett Field, 94035 CA

J. F. Denquin
ICNA/DTIS/ONERA
Salon de Provence, France

Dr. B. Bardy
Research Scientist
EuroMov
Montpellier, France

ABSTRACT

Future vertical lift (FVL) missions will be characterized by increased agility, degraded visual environments (DVE) and optionally piloted vehicles (OPVs). Increased agility will induce more frequent variations of linear and angular accelerations, while DVE will reduce the structure and quality of the out-the-window (OTW) scene. As rotorcrafts become faster and more agile, pilots are expected to navigate at low altitudes while traveling at high speeds. In nap of the earth (NOE) flights, the perception of self-position and orientation provided by visual, vestibular, and proprioceptive cues can vary from moment to moment due to visibility conditions and body alignment as a response to gravitoinertial forces and internally/externally induced perturbations. As a result, erroneous perceptions of the self and the environment can arise, leading ultimately to spatial disorientation (SD). In OPVs conditions, the use of different autopilot modes implies a modification of pilot role from active pilot to systems supervisor. This shift in paradigm, where pilotage is not the primary task, and where feedback from the controls is not available, has consequences. Indeed, space perception and its geometric properties can be strongly modulated by the active or passive nature of the displacement in space. In view of the link between the level of automation and Sense of Agency (SoA), it is of particular interest to examine whether agency mechanisms can modulate the level of visuo-vestibular integration in tasks of action perception and control. An experiment was conducted using the NASA Ames vertical motion simulator (VMS) to evaluate the effects of optical and gravitoinertial cues in the assessment of altitude in contour terrain flight. Seven U.S. Army pilots participated in the experiment. The aim of the proposed research was a) to establish the relative contribution of visual and gravitoinertial cues as a function of the quality of the visual cues (good vs. degraded), and the presence or absence of gravitoinertial cues, b) to determine the role of manual control vs. supervisory monitoring control on the estimation of altitude, and c) study the interactions between the nature and the quality of the sensory cues and the type of control. For the supervisory control condition, the results showed that the gravitoinertial component played a significant role in the estimation of ground height, but only in the case where the optical structure did not efficiently specify the actor-environment interaction. The improvement of the tracking performance in the visuo-vestibular setting as compared to a visual only setting when the visual cues were poor indicates some level of multisensory integration. Preliminary results for the manual control condition suggest the gravitoinertial cues contribute to an increased safety margin in presence of obstacles, particularly in DVE. Altitude accuracy and precision will then be compared for the manual and supervisory control tasks and discussed in the context of the Sense of Agency theory.

INTRODUCTION [1]

This study was a joint effort between the U.S. Army TDD AvMC Aviation and the Office National d' Etudes et de Recherches Aérospatiales (ONERA) in the context of a US/ French Rotorcraft Project Agreement (RPA).

The capability to govern self-motion in rich and changing environments is one of human's most important perceptual–motor skills. Self-motion, whether walking, driving, or flying requires trajectory control while avoiding collisions with obstacles. The perception of self-motion, which includes direction or heading perception and speed, relies on the integration of multiple sensory cues, mostly visual and

Presented at the Vertical Flight Society's 77th Annual Forum & Technology Display, Virtual, May 10-14, 2021. Approved for public release.

This is a work of the U.S. Government and is not subject to copyright protection in the U.S. DISCLAIMER: Reference herein to any specific products does not constitute or imply its endorsement, recommendation, or favoring by the United States Government.

vestibular. Optical patterns specify the position and velocity of distant objects (Refs. 1, 2, 3), while variations in self - motion impact the gravitoinertial field (Refs. 4, 5, 6). Visual motion sensors are tuned to velocity rather than acceleration, and the frequency response of visual motion perception approximates a first-order low pass filter (Ref. 7). Meanwhile, vestibular, and proprioceptive motion sensors are specifically tuned to acceleration (transient movements) and have high-pass filter characteristics (Ref. 8). Under natural conditions, it is always the case that information from several sensory modalities is concurrently available. In the case of self-motion, visual proprioceptive and proprioceptive-vestibular interactions are often casually related. Whereas our perception of position and orientation provided by visual, vestibular, and proprioceptive cues is relatively constant and veridical while on the ground, it can vary from moment to moment in flight due to visibility conditions, body alignment as a response to gravitoinertial forces and internally/ externally induced perturbations. As a result, erroneous perceptions of the self and the environment can arise, leading ultimately to spatial disorientation. For example, erroneous visual perception of distance often occurs during poor visual conditions such as night, whiteout, or brownout. Meanwhile, erroneous perception of motion caused by extreme velocities (too fast or too slow) can result in misinterpretation of directional cues. This is exemplified in the climbing/descending illusion in which a pilot that is accelerating or decelerating can experience the illusion that the aircraft is climbing or diving due to the resultant force being perceived as the force of gravity (Ref. 9). As a result, an inexpert pilot may attempt to make a rectification by pitching the aircraft upward, or worse, downward toward the ground.

The effects of translational and rotational accelerations on the detection of motion and direction while resting immobile, upright, or supine, have been studied extensively in the literature, but little is known when motor control is involved. Most studies of perceived translation have involved the horizontal plane, however, rectilinear vertical acceleration, an inertial stimulation that remains parallel to gravity and alters only the magnitude of background force, has received little attention. In a height control task that considered visual cueing aspects as well as motion, Johnson (Ref. 10) investigated how the displayed visual level of detail (LOD) changes as one gets closer or further away from an object. The results showed that changing the visual LOD to maintain constant global optical density (OD) as the altitude changed, like that of the real world, improved altitude awareness. Separately, adding platform motion improved speed regulation and altitude perception.

To our knowledge, the perception of altitude in low-level flight for a passive observer, i.e., when the pilot is not actively flying, was never investigated. In the context of FVL and OPVs, the use of different autopilot modes will imply a modification of the pilot's role from active pilot to systems supervisor, e.g., air mission commander (AMC). This shift in paradigm, where pilotage is not the primary task, and where feedback from the controls is not available, is not without consequences. Indeed, it has been demonstrated that space perception and its geometric properties can be strongly modulated by the active or passive nature of the displacement in this space (e.g., Refs. 11, 12). While the question of being an active vs. a passive operator has regarding the perception of ego motion in specific gravitational and visual conditions has been largely unexplored, it can be investigated using the theoretical frame of "agency". Sense of Agency refers to one's ability to control his/her actions and, through them, events in the external world (Refs. 13, 14). In the context of automation and human-computer interactions, the question of agency, i.e., the perception of the level of control that we have on these systems, is central (Ref. 15). Because automation can fail, and because the AMC must maintain a holistic situation awareness (HSA), it is critical to understand how visual and gravitoinertial cues contribute to the perception of self-motion when the pilot is not an active agent, and when attention may be divided between tasks. In the case of low-level flight such as nap of the earth (NOE) missions, the perception of height is critical as flying too high can lead to aircraft detection by the enemy's radars and flying too low can lead to controlled flight into terrain (CFIT) or collision with an obstacle. Optimal perception of height relies on the synergistic contribution of multiple senses, mostly the visual and the vestibular systems, the role of each and their interactions detailed in the next sections.

Optical information and the visual system

The human visual system is composed of two complementary sub-systems, the ambient visual system which enables orientation relative to the global environment, and the focal visual system, allowing orientation relative to an object (Refs. 1, 16, 17, 18). Gibson (Ref. 1) has shown first that the direction of self-motion can be derived from the motion pattern of texture points in the visual field. He showed that for an observer in rectilinear motion, the "optical flow field" or "streamer" pattern seems to expand from a focal point that indicates the direction of motion. The optical flow generated at the pilot's observation point contains crucial information for controlling self-motion (Refs. 1, 19). One of the most important components of the optical flow field structure is motion parallax, which informs about relative distance (Ref. 1) and egocentric distance (Ref. 20), and strongly depends on the ground texture.

Visual cues for altitude perception in Flight

A two-dimensional (2D) texture on a flat terrain surface provides two types of cues for NOE flight: 1) the *depression angle*, which is the visual angle formed by the horizon and a terrain edge that is oriented perpendicularly to the direction of motion and 2) the *optical splay angle*, which is the visual angle formed by the motion path and a terrain edge oriented parallel to the direction of motion at the convergence point on the horizon (Ref. 21). However, it is unclear how to define splay and depression angles when the terrain consists of randomly placed three-dimensional (3D) objects and how they contribute to the perception of altitude when other cues, such as visual occlusion cues are more salient. On the

simulated terrain shown in Figure 1 extracted from the video of an experimental trial, there are no clear terrain edges oriented perpendicularly or parallel to the path of travel. Optical splay angle and depression angle have been proposed as quasi-independent sources of information about speed and altitude (Refs. 22, 23, 24). Both splay angle and depression angle are components of an expansion of texture that is associated with the approach to a surface or time to contact, *tau* (Refs. 25, 26).

Another visual cue that could be used for altitude maintenance is the change in the *optical flow rate* (ground rush) which is a measure related to the angular speed (splay angle) of terrain elements (trees, fields, etc.) as one moves through a visual scene. The rate of change of size is proportional to the rate of change of altitude (Ref. 23). Similarly, *optical edge rate* (also referred to as texture rate) is the rate at which texture elements pass a reference point that is fixed relative to the observer. The rate at which depression angle changes is affected both by altitude and forward speed. Texture rate yields a good estimation of ground speed when the spacing between these elements remains relatively constant. Thus, changes in flow rate can veridically signal altitude deviation when texture rate is constant. Although edge rate does not change with altitude, it can affect the perception of self-motion (Ref. 27), which may interact with perceived texture density and optical flow rate. Evidence for interaction among visual cues to altitude has been reported by Flach et al. (Ref. 21).

Global optical density (OD) (perceived ground texture density) has been defined by Owen and Warren (Ref. 22) as "the number of ground elements required to span one eye-height distance". For a constant texture size, changes in altitude will result in proportional changes in OD (Ref. 28). Assuming that actual texture density is constant, the perceived texture density will increase as altitude increases, as seen in Figure 1. In the case of movement over a textured surface or a scene containing 3D objects, the most salient perceptual cue is the motion gradient formed by differential movements of the texture elements or the 3D objects (Ref. 29). Patterson et al. suggested that motion gradient is a visual cue that can be used for altitude maintenance (Ref. 30).

Motion perspective, as conceptualized by Gibson (Ref. 1), is another cue that may be relevant to altitude control in NOE. Motion perspective refers to the relative movements of objects that occurs when the observer moves and is a consequence of the fact that nearer objects move faster across the retina than do farther objects. There is some evidence that vertical motion-perspective cues may be used for altitude control (Ref. 30). Optical flow is the logical extension of motion perspective (parallax) to all points in a scene (see Figure 2). The role of *visual occlusion* as a cue to altitude maintenance in low-altitude flight has been rarely investigated. Leung and Malik (Ref. 31) showed that the amount of visual occlusion present in a scene made up of 3D objects oriented perpendicularly to the ground is related to the product of object height, object density and object radius.

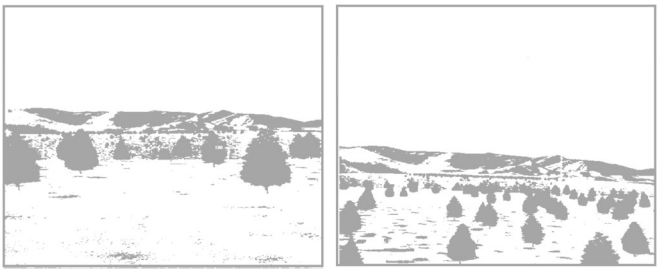

Figure 1. The same scene extracted from an experimental video trial in good visual environment (GVE) at 27 ft above ground level (AGL) on the left and 63 ft AGL on the right. Because the actual texture density is constant, the perceived texture density increases as altitude increases.

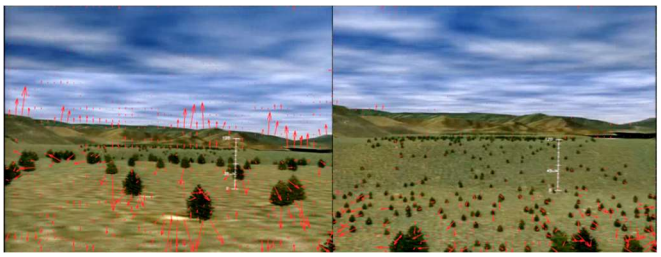

Figure 2. Example of out-the-window optical fields in GVE as a function of altitude. Left: 27ft AGL. Right: 63 ft AGL.

In a simulated altitude maintenance task, Gray et al. (Ref. 32) showed that participants were using changes in the magnitude of visual occlusion (i.e., changes in the amount of visible ground surface between trees) as a visual cue.

Vision for Perception and Vision for Action

It has been proposed (Refs. 26, 33, 34) that the visual perception of objects and the visual control of action relies on relatively different neural pathways, respectively the ventral stream and the dorsal stream. These two streams differ in the metrics of interest (Ref. 33). Vision for perception relies on the relative size of objects (relative metric) and vision for action on their physical size (absolute metric) (Ref. 34). This aspect is important to consider in the context of SoA and could have implications for the perception of altitude during as a function of the nature of ego-motion in flight, i.e., active vs. passive.

Visual illusions

Even during natural flight in a 3D environment, and despite providing the most important information to maintain spatial orientation with respect to the terrestrial frame of reference, visual orientation can be biased. The importance of vision to self-motion perception is clear when considering the effects of degraded or disrupted vision during self-motion. For instance, pilots flying in DVE, deprived from visual Earth-based orientation cues, could be prone to orientation errors if they do not rely on instruments. One example is the *illusion of self-motion* (e.g., vection, Refs. 35, 36, 37) occurring (but

not only) when pilots misinterpret peripherical visual stimulation, often due to surrounding objects moving at different speeds or in a different direction, or to rotating light (e.g., reflection of aircraft's rotors or ground lights). Another illustration is the *illusion of height* (Refs. 37, 38), that occurs during flight over featureless terrain where few visual cues are available. This can give an illusion of lack of movement since the normal passage of visual details is missing (poor optical structure). It can also give the pilots a false sense of their height above ground, and lead to CFIT. In most cases, these misperceptions are benign, short in time, and easily compensated for thanks to the contribution of the vestibular system (Ref. 39) and visuo-vestibular interactions (Ref. 40).

Gravitoinertial (GI) information and the vestibular system

The vestibular system is the most influential of the non-visual senses for the detection of information about passive and active, linear, and angular self-accelerations (Ref. 41). The vestibular system generates information for the three axes of head translation (transverse, longitudinal and sagittal) and the rotation, and provides spatial orientation in relation to the vertical gravity. Located at the level of the inner ear, the vestibular system consists of five distinct organs: the three semi-circular channels (sensitive to angular accelerations; head rotations) and the two otolithic organs (saccule, utricle) which are sensitive to linear accelerations and gravity. Beyond this anatomical aspect, it is important to note that vestibular integration has the distinction of being intrinsically multisensory (Ref. 42). There is no primary vestibular cortex per se, and there is more of a network of vestibular areas interconnected with the parieto-vestibulo-insular cortex (PVIC) (Ref. 43). Thus, the vestibular sensory dimension is essential to a set of processes essential for movement perception such as vision stabilization (vestibulo-ocular reflex, VOR), balance maintenance and head orientation estimation. In addition to providing consistency with visual, proprioceptive, and auditory inputs, the vestibular system allows self-motion to be discriminated from an external movement. Also, the weight of one sensory information compared to another depends on environmental constraints (gravitoinertial, optical) and the nature of the task (intentional control, automation, etc.).

Visuo-vestibular interactions

The relation between optical changes (detected by the visual system) and inertial changes (detected by the vestibular system) during self-motion has been widely investigated (Refs. 44, 45) and studies have shown the importance of spatiotemporally coherent visuo-vestibular cues for successful control of self-motion (Refs. 5, 46). However, discrepancies (e.g., non-coherence or noise) in the ambient arrays can lead to an erroneous sense of height, orientation, or speed, with dramatic consequences such as loss of control. Decreasing altitude in a helicopter generates both optical (e.g., variations in the flow structure) and inertial (variations in the GI structure) changes. In a nominal situation (e.g., no wind, good weather, daylight) variations in optical and GI structures are continuously congruent. But in more challenging situations, such as when landing in a desert, the sand lifted by the rotors often creates a condition in which ground textural cues are absent and the horizon is indistinguishable (Ref. 47). This sudden interruption of visual stimulation without affecting vestibular stimulation creates unnatural covariations between the two senses, and in this context, pilots are often unable to efficiently control their altitude and self-motion (Ref. 48). These observations are theoretically grounded into two approaches, the sensory integration approach, and the ecological approach. According to the sensory integration approach, the various cues sampled by our senses are combined to produce an integrated percept allowing us to successfully interact with our environment. Because of the variability of sensory cue reliability (due to environmental variations, or errors in sensory detection), this theoretical framework proposes that cue integration depends on probabilistic inferences (Ref. 49). One version of this approach is the sensory weighted approach, which proposes that each sensory cue is weighted based on this reliability, and that weight depends on integration patterns derived from the Bayesian probability theory (Refs. 6, 50, 51, 52).

In the ecological approach, the interaction with the environment is directly specified in the covariations of the flow structures detected by the various senses. The intermodal theory of perception (Ref. 53) proposes that variations in the optical structure reaching the eyes of the pilot and variations in the gravitoinertial structure stimulating their vestibular system are simultaneously specified in a higher-order structure called the Global Array (GA). The GA is a structure that extends across multiple forms of ambient energy. Higher-order invariants existing in the GA have been demonstrated to be responsible for the perception and control of reaching (Ref. 20), but to our knowledge it remains to be discovered in the context of NOE flight. Nevertheless, and in the case of ego motion, visual information is physiologically dominant, but it is now established that the vestibular system plays a key role in the determination of this type of action (Refs. 45, 54). In 2010, Fetsch (ref. 44) explored visuo-vestibular integration by introducing disparities in vestibular inputs (moving platform) and visual inputs (optical flow). They demonstrated a weighting of visuo-vestibular sensory inputs according to their reliability. More specifically, they showed that vestibular information is attenuated when the visual information is of high relevance for body movement coding summation (see also modality appropriateness hypothesis for vision and audition, Ref. 54, 55).

Thus, in good visual environment (GVE) conditions, the visual information available in the external environment can be sufficient for the pilot to characterize his own movement and attitudes with respect to the terrestrial reference. On the other hand, in DVE conditions, when visual information can be very limited (e. g., entry into a cloud layer, night or brownout), the acquisition of information about the terrestrial reference is hindered and even the most experienced pilot may be unable to properly assess (consciously or not) the attitudes of his aircraft. Furthermore, the reliability (signal-to-noise

ratio) of these cues can vary rapidly and unpredictably, because of environment changes or because of sensory encoding error. If, from an evolutionary point of view, the vestibular system is completely adapted to the earth's motion, it does not follow that it is well-adapted to the aeronautical environment and may constitute a major physiological component of the SD (Ref. 56). SD is therefore due to the functional inability of the vestibular system to inform the operator about his/her own motion when visual information is insufficient, given certain kinetic condition. Furthermore, visuo-vestibular integration is a multisensoriality topic that is relevant to numerous aeronautical domains.

Automation and Sense of Agency

While automatic flight control systems can increase safety through workload reduction, empirical data also suggests that it could have negative performance and safety consequences for the pilots, a set of difficulties called the out-of-the-loop (OOTL) performance problem (Refs. 57, 58, 59). OOTL performance problem is fundamentally an issue of human-automation interaction and can arise because of issues of poor performing monitoring, impaired decision-making (Ref. 60), and reduced perception, i.e., lack of operator sensitivity to signal (Ref. 61).

SOA and consciously perceived control over the immediate environment

A direct consequence of the OOTL phenomenon is a reduction of the "Sense of Agency" (SoA), i.e. the experience of being in control both of one's own actions and, through them, of events in the external world (Refs. 13, 14, 62). The SoA can be subdivided into a sense of intentionality or intentional causation, a sense of initiation and a sense of control (Ref. 63). It raises the question of how pilots perceive their agency in the context of human-machine interaction and collaborative control. Of particular interest for FVL, is how the SoA might affect the perception of self-motion (perception of egocentric distance, direction) in rapidly/ unpredictably changing environments.

In the aviation domain, Berberian et al. (Ref. 15) investigated the participants' SoA when performing an aircraft supervision task using a flight simulator under different levels of automation. The task required the participant to observe a flight plan and after a random time interval, a conflict occurred due to the presence of another plane. The participant was asked to take an appropriate action and implement it using a button-based interface. The authors found a decrease in the SoA (for both implicit and explicit measures) associated to the increase in automation. They argued that the increasing level of automation tends to distract operators from action outcomes, decrease their sense of control and therefore disrupt their overall performance. Further empirical evidence comes from Coyle et al. (Ref. 64). In a machine-assisted point-and-click task, these authors explore how the assistance given to participants could influence the user's SoA. They showed that, up to a certain point, the computer could assist users while also allowing them to maintain a sense of control and ownership of their actions and the outcomes of those actions. However, their results suggested that beyond a certain level of assistance users experienced a detectable loss in their sense of agency. Taken together, these studies indicate that automation technology could disturb the mechanism underlying the SoA. This decrease in agency could generate critical concern regarding both automation acceptability and operator behavior.

The study

Testing the visual (optical) and vestibular (gravitoinertial) contributions and their interactions in a successful performance during NOE flight requires manipulating the perceptual environment of the pilot. Due to the high-risk level and the difficulty in controlling environmental variables (e.g., wind or luminosity), this manipulation is difficult in real life. Motion-based flight simulators are widely used to provide an experimentally controlled environment. They can recreate, to a certain extent, natural flying scenarios with (limited) inertial and optical changes. The NASA Ames vertical motion VMS provided the ideal platform to evaluate the contribution of optical and gravitoinertial information, as well as their interactions, on the perception of altitude.

Two conditions were tested. In the first condition, referred to as Supervisory Control condition, pilots were asked to passively report their perceived altitude above the ground level (AGL) while moving in a simulated NOE flight in autopilot (AP) mode. In the second condition, referred to as Active Control condition, the pilots had to actively regulate their altitude, speed and heading as if they were in a real NOE situation.

These two conditions require different perception mechanisms. In the Supervisory Control Task, the representation of the self in the environment relies on the integration of relative cues during visual *perception decoupled from action*, where the pilot is experiencing a reduced Sense of Agency. Conversely, in the Active Control Task, the representation of the self in the environment is mediated by *control-oriented action-perception* mechanisms, where the pilot has a strong sense of control.

In GVE, where the visual cues are highly reliable, one may expect no or a very low level of contribution of the gravitoinertial cues to altitude perception. Conversely, in DVE, the reliability of the visual cues decreases, and the contribution of the gravitoinertial cues is expected to increase and should give rise to some level of multisensory enhancement.

Here, we present the results of the Active Control condition flown at 55 knots and compare the results with the Supervisory Control condition. Assuming transitivity between passive and active observer perceptive mechanisms, the hypothesis was that pilots would produce a better performance in the presence of congruent visual and gravitoinertial stimulation rather than during visual stimulation alone. It was also posited that when the visual information was compromised in DVE or when flying higher,

the contribution of the gravitoinertial cues would be more heavily weighted.

Methods

Participants

A total of seven male pilots from the U.S. Army (one research instructor pilot, three experimental test pilots, two research pilots and one instructor pilot) aged 27 to 57 (mean 37.5 years) participated in the experiment. Flight hours varied between 560 hours and 7300 hours (mean 2736 hours) and simulator experience between 100 hours and 1000 hours (mean 365 hours). All had flown night vision googles (NVG)/ DVE conditions (40 to 1500 hours, mean 765 hours).

The Simulator

The experiment was carried out on the NASA Ames Research Center VMS, an uncoupled six-degree-of-freedom (6 DOF) (three translational and three rotational) motion simulator (Figures 3, 4, 5). The distinctive feature of the VMS is its unequaled large amplitude, high fidelity motion capability. It was equipped with a R-cabin emulating a utility class UH-60 sized helicopter, with an OTW FOV representative of that class of vehicle. Two gravitoinertial conditions were tested, one with cabin motion (the gravitoinertial profile is the double derivative of the terrain profile) and one without cabin motion (the visual environment only is optically in motion).

The Visual Display

The OTW visual scene was generated by a Rockwell-Collins EPX-5000 image generation system providing a high-resolution visual environment at update rates ≥60Hz. The visual scene was presented on the cockpit top three windows (the chin window was not used to prevent the ground from being viewed and used to judge the altitude). The horizontal FOV spanned +-78 degrees and the vertical FOV covered -16 to +12 degrees, as shown in Figure 4.

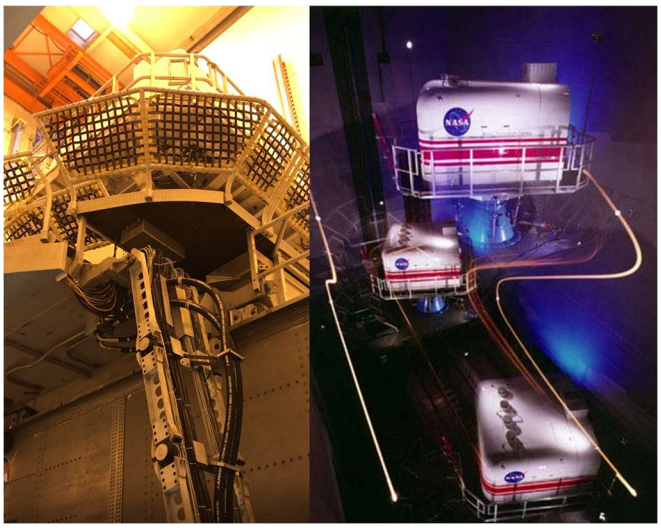

Figure 3. NASA Ames 6 DOF Vertical Motion Simulator.

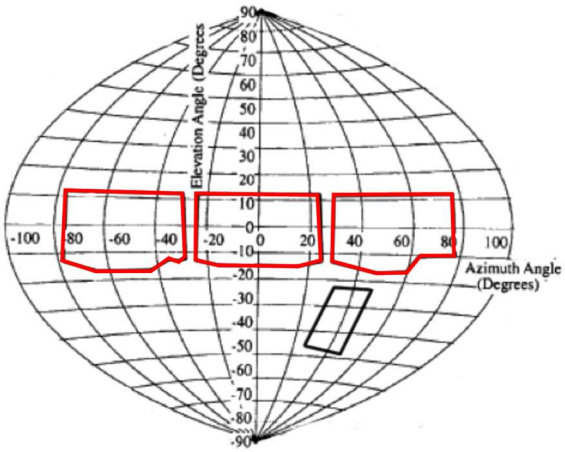

Figure 4. VMS R Cab cockpit Field of view.

Figure 5. VMS R Cab cockpit emulating a utility class UH-60 sized helicopter.

The Virtual Environment

The virtual visual environment characteristics, terrain profile, flight and perturbation/obstacle parameters are illustrated in Figures 6 and 7 and summarized in Table 1.

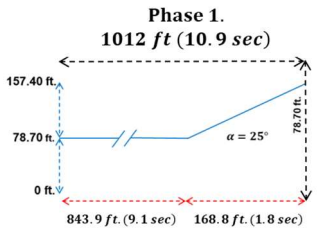

Figure 6: Terrain profile for phase 1 (distance travelled at 55 knots).

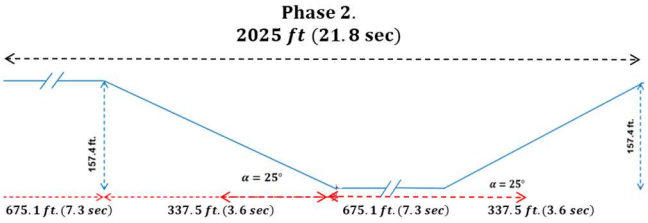

Figure 7: Terrain profile for phase 2, 1 block, repeated 3 times (distance travelled at 55 knots).

Table 1. Visual Environment, Terrain and Flight Characteristics.

Parameters	
Tree height (all same color)	18 $ft.$ (+/- 1 ft.)
Tree canopy diameter	15 $ft.$ (+/- 1ft.)
Tree density	193/square mile
Height (altitude) initialization (Pilot eye-level)	$45ft.$ $(2.5\ trees)\ AGL \pm random * 4.5$ with $0 \leq random \geq 1$
Height (altitude) above tree	$27ft.$
Phase 1: Plateau altitude	$78.7ft$
Phase 1: Plateau length	843.9 $ft.$ (9.1 sec)
Phase 1: Ascent length/ angle of attack	168.78 $ft.$ (sec), 25°
Phase 2: Plateau low	0 $ft.$
Phase 2: Plateau high	157.4 $ft.$
Phase 2: Plateau length	675.12 $ft.$ (10 sec)
Phase 2: Ascent/ Descent length/ angle of attack	168.78 $ft.$ (sec), 25°
Supervisory Control Task: perturbation magnitude and direction (Upward vs. Downward), randomly presented 10 to 55 sec after the beginning of Phase 2)	$\pm$18 $ft.$ (+/- 1 ft.), randomly occurring within a descent (DOWN), low plateau (PL) or ascent (UP) segment
Active Control Task: obstacle powerline locus	Height 18 ft, randomly positioned within a descent (DOWN), low plateau (PL) or ascent (UP) segment
Initial speed	35 kts, 55 kts
Block trial length	6413.67 $ft.$, $\approx$ 90 sec at $\approx$ 55 kts

Phase 1 initiates the flight level (45ft +/- 10%) and speed (35 or 55 kts). The virtual environment started as a flat ground surface followed by a short ascent that ended Phase 1. This phase was followed by a succession of high plateau (PH) Descent (DOWN), low plateau (PL) and Ascent (UP) over 2025 ft (phase 2), forming a cycle repeated three times in the passive condition and approximately three times in the active condition, given the speed variations. Trials lasted on average 90 sec.

Visual cues

In the GVE condition, all the visual cues are available to the pilot. In the DVE condition, the visibility level was degraded with fog and set at ¼ mile, which decreased the structure and the quality of the OTW cues (optically relevant primitives). Because heading was maintained relatively constant (rectilinear motion), and no pitch was involved, the optical flow field was generated by a strictly forward translation. Therefore, the variations in the optical flow field were only induced by the terrain variations (plateau, ascent, descent), the meteorological conditions (GVE vs. DVE), and the flight level (see Figure 8).

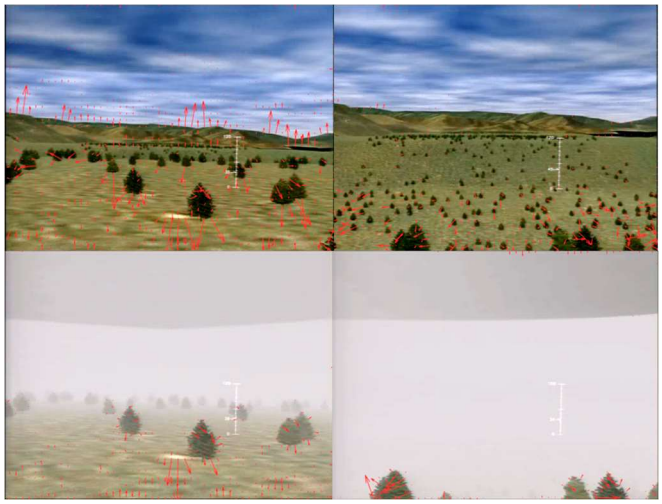

Figure 8. Example of out-the-window optical fields as a function of altitude. Top to Bottom: GVE and DVE. Left to Right: 27ft AGL and 63 ft AGL. Optical vector fields (red arrows) are superimposed on the simulation image to illustrate the differences in visual cues available in the different configurations.

Previous research has shown that performance in simulated NOE tasks (altitude maintenance) is related to variations in global object density, object height an object radius (Refs. 28, 32). To control for these effects, the terrain was populated with 193 identical trees per square mile randomly distributed (Figure 8) to maintain the same density gradient (number of trees per degree of visual angle) throughout the entire trial. The trees height and canopy diameter were maintained constant to prevent differences in the magnitude of visual occlusion (refer to Table 1 for details). A patched texture was layered over the profile. A mountainous background surrounded the experimental environment.

Gravitoinertial cues

Two gravitoinertial conditions were tested, one with cabin motion (the gravitoinertial profile is the double derivative of

the terrain profile) and one without cabin motion (the visual environment is only optically in motion). In the Supervisory Control condition, an unknown (to the pilot) forcing function (sum of sines, SOS) is introduced after a random delay.

Experimental Test Matrix

The experiment followed a full-factorial repeated-measures design (all the pilots experienced all the conditions) with two within subject factors, Visibility (GVE, DVE) and Cabin Motion (ON, OFF), giving rise to 4 experimental blocks: Visual [GVE, DVE] * Gravitoinertial [Cabin motion ON, Cabin motion OFF] (see Table 2). Each block contained 10 trials (5 at 35 kts, 5 at 55 kts). The experiment consisted of 20 trials per participant, each block (Visibility * Gravitoinertial) counterbalanced between participants. Each trial lasted on average 2 minutes (90 seconds trial + reconfiguration). Pilots were encouraged to take five minutes breaks between blocks (10 trials). Active Control and Supervisory Control blocs were randomized.
For each trial and each pilot, the initial flight level (pilot's eye level) was set to a randomized value of 45 ft AGL +/- (4.5 ft * random), with 0<=random<=1; min=40.51, max=49.44. Initial speed was set at 57 kts.

Table 2. Experimental Design: two experimental conditions (Supervisory vs. Active Control), two levels of visual environment (GVE vs. DVE), two levels of gravitoinertial environment (Cabin Motion ON, Cabin Motion OFF). The results presented here are for the 55 kts condition. Five repetitions were performed randomly between conditions for each configuration. Active Control and Supervisory Control blocs were randomized.

	Supervisory Control Task				Active Control Task			
	GVE		DVE		GVE		DVE	
	35	*55*	*35*	*55*	*35*	*55*	*35*	*55*
GI ON	5	5	5	5	5	5	5	5
GI OFF	5	5	5	5	5	5	5	5

The tasks

The two experiments required different perceptive-motor mechanisms. The Supervisory Control task relies on the integration of relative cues during perception *decoupled from action*, while the Manual Control task involves a *continuous control-oriented action-perception* task.

Supervisory Control task

In the Supervisory Control task, the pilots were passive observers of a pseudo automated NOE flight. They had no control over the simulated motion. They were instructed that they were observing a pre-recorded flight with inherent small variations in height, and that an 18ft vertical perturbation, upward or downward simulating a vertical wind shift would be introduced during the Phase 2 of the flight (Figure 9, top). Their task was to report their perceived height above the ground using a cursor on a vertical tape, from 0ft to 120 ft, displayed on the display window, controlled by the collective position. The tape was located 45 degrees and 5.25 inches from the center of the FOV (lower right quadrant, see Figure 9 bottom). At the beginning of the trial, the aircraft position was set at a random height (45 ft +/- 4.5 ft) unknown to the pilot. The cursor's initial position was also set at a random position (45 ft +/- 4.5 ft), uncorrelated to the aircraft's initial altitude. Pilots had no access to instruments.

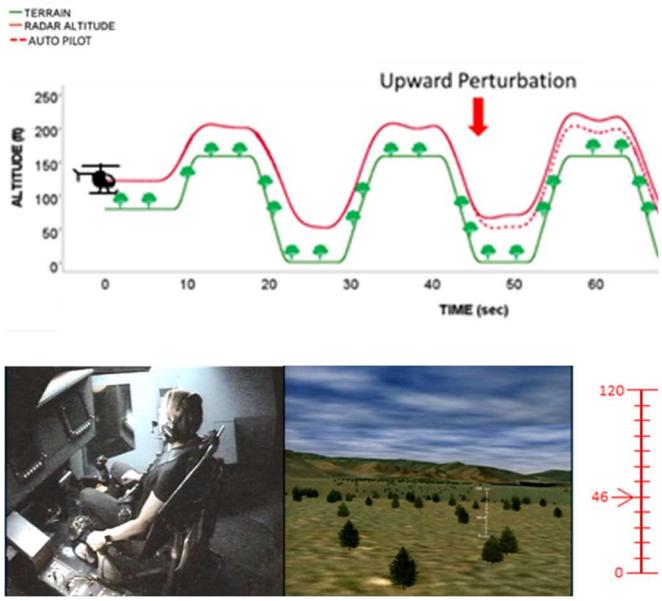

Figure 9: Supervisory Control task. Top: Terrain profile with a Upward perturbation. Bottom: Participant in situ using a cursor on a vertical tape displayed on the display window to report his perceived altitude. The cursor was controlled by the collective position.

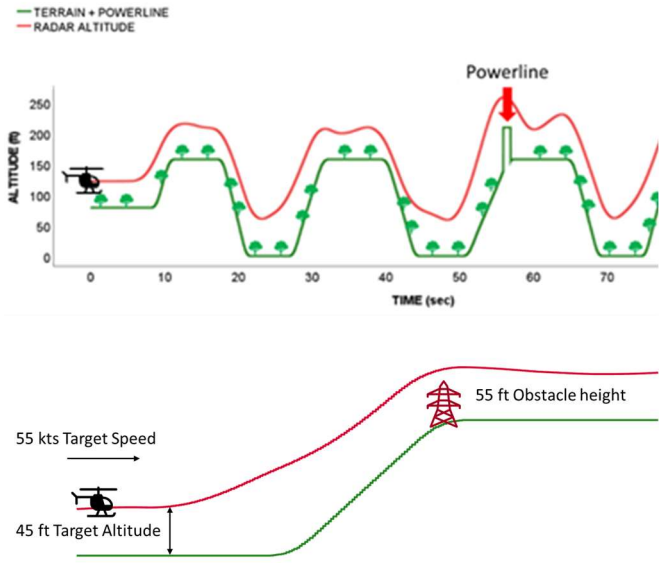

Figure 10: Active Control task. Terrain profile with the 55ft high obstacle powerline loacted at the end of an ascent. Target speed was set at 55kts, target altitude was set at 45ft AGL.

Active Control task

In the Active Control task, pilots were instructed to fly above the terrain at a constant 45 ft altitude and constant speed of 55 knots while keeping the heading constant. After a random delay, pilots had to climb over a 55 ft powerline (Figure 9, middle and bottom), before returning to their initial flight level, speed and heading as soon as possible. The Powerline Obstacle was located either on a DOWN, PL or UP terrain segment. Pilots had no access to instruments.

Height estimation as a function of the terrain profile

Height estimation over flat textured terrain is relatively easy and altitude and perceptual resolution are roughly inversely related.
Estimating height above sloped terrain during ascent is the most challenging as it requires: 1) Distance estimation from the nearest visible point on the slope; 2) Estimation of the slope associated with the reference point established in (1); 3) Recollection of the terrain contour that is no longer in view when the gradient of that terrain changes from level to sloped; 4) Mental projection of distance along the overrun (unseen) terrain contour based on perceived groundspeed. Height estimation when established in a descent is also challenging, requiring: 1) Recollection of the terrain contour that is no longer in view when the gradient of that terrain changes from level to sloped; 2) Mental projection of horizontal distance flown beyond the crest of the hill until the descent begins; 3) Estimation of descent rate based on distant line of sight (LOS) cues groundspeed (see Figure 8 bottom); 4) Integrating #2 and #3. Because the slope during the descent is never in view, height can only be inferred via #4 and prone to inaccurate height perception. Hill climb and descent maneuvers will therefore exhibit different characteristics resulting from the modifications of the optical flow (Ref. Padfield).
When a pilot is approaching an obstacle, the affordances of the environment (i.e., the perceived opportunities for interactions, see Ref. Gibson) are guiding the choice of action to takes, such as pulling up and climbing over the obstacle, finding a way around, or coming to a stop. Although Segment type was initially considered as a controlled variable, it became evident during the empirical examination of the data that it should be considered as an independent visual variable, since each segment generates an idiosyncratic optic flow field.

Independent Variables

The independent variables for the Active Control Task were Cycle, Segment type, Visibility and Motion (see Experimental Test Matrix section for Visibility and Motion).

Cycle and Segment type

To compare Radar Altitude, Forward Speed and Heading with and without the presence of an obstacle, the runs were decomposed into three cycles determined by the location of the powerline. A pre-obstacle region (referred to as Cycle 0, C0) and a post-obstacle region referred to as Cycle 2 (C2) were determined based on locus of the powerline obstacle.

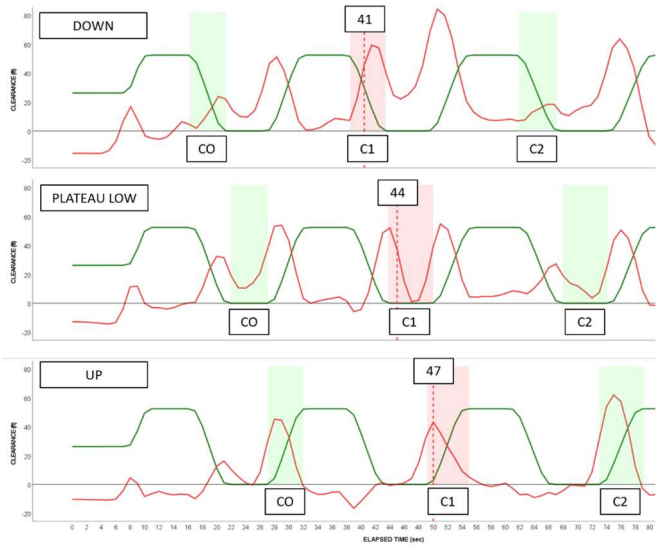

Figure 10: Clearance (ft above powerline altitude) superimposed over terrain profile (ft/3) for from top to bottom: DOWN Segment, Plateau Low (PL) Segment and UP Segment. Obstacle times were respectively 41 sec, 44 sec and 47 sec after the beginning of the trial. Pre-obstacle (C0), obstacle (C1) and post-obstacle Cycles (C2) were used to compare the performance for a similar segment of terrain.

For example, if the powerline was located on a descent (DOWN), the performance was compared for the DOWN segments only. Figure 10 illustrates from top to bottom, the methodology for a DOWN, PL and UP segment. Obstacle times were respectively 41 sec, 44 sec and 47 sec after the beginning of the trial. The cycle of reference, C1, is indicated by a red window, the pre- (C0) and post-obstacle (C2) cycles are indicated by a green window.

Dependent Variables: Quantitative Measures of Performance

Assessing nominal flight performance and performance post obstacle.

As a preliminary analysis, nominal flight performance and the capacity to regain initial altitude and ground speed after clearing the powerline obstacle was examined. Specifically, speed, radar error and heading error were compared between C0 and C1, as a function of Segment, Visibility and Motion.

Assessing the flight performance at the time of the powerline obstacle

The analysis of the maneuver strategy was analyzed within the segment of reference (C1) from:

- Clearance magnitude at the locus of the Obstacle (see Figure 11, #1)
- Maximum Clearance magnitude (see Figure 11, #2). Maximum Clearance magnitude was determined at the locus of reversal from positive to negative altitude. Note that in some instances, the Maximum clearance was observed outside the segment.

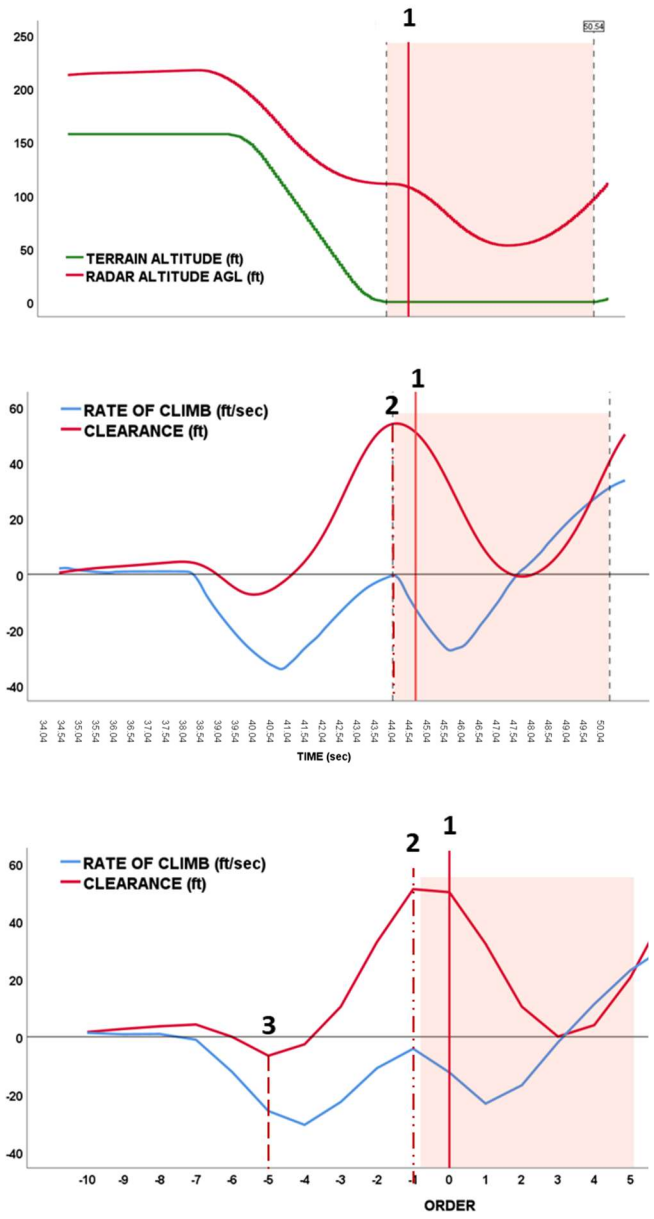

Figure 11: Pilot P2, GVE, Cabin Motion OFF. Top: Radar altitude AGL over terrain, with powerline obstacle (#1) located 69 sec after the beginning of a PL segment. The segment is highlighted with a red window. Middle: Clearance and rate of climb, with powerline obstacle (#1) and Max Clearance (#2). Bottom: Powerline locus (#1), Maximum Clearance (#2) and Pull-up initiation time (#3).

- Pull-up initiation Time (Figure 11, #3). The locus of altitude reversal from negative to positive was used to determine the *time of maneuver initiation* (pull-up). Sustained, monotonous increase in altitude were identified, their starting point determining the time of maneuver onset. Because it is reasonable, for a 55 kts forward speed, to expect an avoidance maneuver starting between 10 sec (825 ft) and 4 sec ($\cong 330\ ft$) prior to the obstacle, a 10 sec analysis window was selected to identify the locus of reversal. When the reversal was located outside the segment of reference, the time of maneuver initiation was determined with a 1sec resolution using a discretized range.
- Time and magnitude differences between Obstacle Clearance and Max Clearance (#1- #2).

RESULTS

The normality of data (Clearance magnitude, Maximum Clearance Magnitude and Time, Time of Maneuver initiation) was tested using Shapiro-Wilkinson procedure for each experimental condition, resulting in twelve test outcomes per dependent measure. Rejection of the null hypothesis was accepted if 25% or more of the tests were significant at $\alpha = .05$). Time of avoidance maneuver initiation, as computed from the clearance reversals and polarity showed at least 25% of non-normal distributions. For normally distributed data, two and three-way Analyses of Variance (ANOVA, Univariate and Repeated-Measures) were used. For Univariate ANOVAs, post-hoc LSD tests were used for pairwise comparisons. For repeated-measures ANOVAs, Bonferroni post-hoc tests were selected. Chi-Squares Tests of independence were used to estimate the differences in distribution between categorical data. For non-normally distributed data, non-parametric related-sample tests were used (Friedman Test and Wilcoxon Signed Ranks Test). Obstacle Clearance, Maximum Clearance, and their derivatives (differences in time and magnitude) were averaged over a 150 msec window. All the effects described here were statistically significant at $p < 0.05$ or better.

Assessing nominal flight performance and performance post obstacle.

Figure 13 shows an example fly over clearance trajectory in a descent, with (C1) and without obstacle (C0, C2). The trajectories have overlapping for illustration purposes.

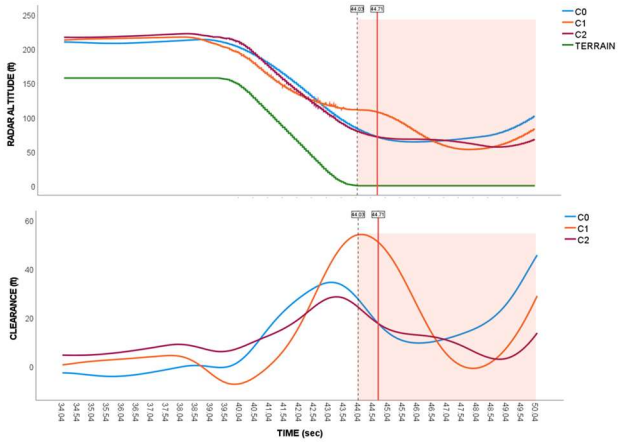

Figure 12: Clearance trajectory for a DOWN segment with (C1) and without obstacle (C0, C2). GVE, Cabin Motion OFF.

Ground Speed

A repeated Measures ANOVA with Cycle as within subject variable and Segment, Motion, and Visibility as between subject factors showed a significant effect of Cycle on Ground Speed ($F_{2,246} = 51.62, p < .0001$), a significant effect of segment ($F_{2,123} = 3.14, p = .04$) and a significant effect of Motion ($F_{1,123} = 9.78, p = .002$). There was no significant effect of interaction. The Initial ground speed was fixed at 57.27 ft for all pilots and all conditions. Ground speed significantly decreased between C0 ($\mu = 54.76, SE = .22$) and C1 ($\mu = 51.33, SE = .49$) (C0,C1: $F_{1,123} = 80.66, p < .0001$) and C1 and C2 ($\mu = 50.13, SE = .63$) (C1,C2: $F_{1,123} = 7.01, p = .0009$). The difference in ground speed was not different between DOWN and PL segments (DOWN: $\mu = 53.02, SE = .71$; PL: $\mu = 52.58, SE = .58$; Multiple Comparisons: DOWN,PL: $t = -.01, p = .98$), but was significantly lower for UP segments than for DOWN and PL segments (UP: $\mu = 50.61, SE = .74$; DOWN,UP: $t = 2.11, p = .02$; PL,UP: $t = 2.13, p = .01$) Last, ground speed was significantly lower when gravitoinertial cues were available (i.e. Cabin Motion ON) (Cabin Motion OFF: $\mu = 51.47, SD = 5.47$; Cabin Motion ON: $\mu = 48.77, SD = 6.03$).

Radar Altitude

A repeated Measures ANOVA with Cycle as within subject variable and Segment, Motion, and Visibility as between subject factors showed a significant effect of Cycle on Radar Altitude (ft AGL) ($F_{2,246} = 51.62, p < .0001$), a significant effect of segment ($F_{2,123} = 19.69, p < .0001$), a significant effect of Motion ($F_{1,123} = 7.84, p = .006$), and a significant effect of Visibility ($F_{2,123} = 11.17, p = .001$). The effect of interaction between Cycle and Motion was marginally significant ($F_{2,246} = 2.98, p = .05$).

As expected, Radar Altitude increased significantly between C0 and C1 (C0: $\mu = 69.07, SE = 1.21$; C1: $\mu = 84.08, SE = 1.59$; $t = -15.07, p < .0001$) and return to a significantly lower level during C2 than during C0 (C2: $\mu = 65.61, SE = 1.47$;C0,C1: $t = 3.39, p = .002$). Radar altitude was higher with than without gravitoinertial cues (Cabin Motion OFF: $\mu = 69.61, SE = 1.61$; Cabin Motion ON: $\mu = 76.18, SE = 1.69$), and lower in GVE than in DVE (GVE: $\mu = 68.98, SE = 1.61$; DVE: $\mu = 76.81, SE = 1.69$).

Overall, Radar Altitude was not significantly different between DOWN and PL segments (DOWN: $\mu = 70.02, SE = 2.12$; PL: $\mu = 65.62, SE = 1.72$; DOWN,PL: $t = 4.39, p = .11$), but was significantly higher for UP segments (UP: $\mu = 83.04, SE = 2.20$; DOWN,UP: $t = -13.01, p < .0001$; PL,UP: $t = -17.41, p < .0001$).

Radar Altitude was not statistically different as a function of Motion for C0 and C1 (C0: OFF: $\mu = 65.69, SE = 1.8$; ON: $\mu = 69.99, SE = 1.84$; OFF,ON: $t = -4.30, p = .09$; C2: OFF: $\mu = 62.26, SE = 2.20$; ON: $\mu = 65.87, SE = 2.28$; OFF,ON: $t = -3.6, p = .25$). Conversely, radar altitude was significantly higher with cabin Motion On during C1 (OFF: $\mu = 76.77, SE = 2.24$; ON: $\mu = 86.35, SE = 2.29$; OFF, ON: $t = 3.21, p < .003$).

Pull-Up Initiation Time

The observed times of sustained clearance reversals, averaged by Segment, Visibility and Motion conditions are plotted in Figure 13. As expected, the Segment type had a significant effect on pull-up initiation time ($x_2^2 = 13, p = .002$). The maneuver was initiated earlier for the UP segments ($\mu = -6.52, SD = 1.09$) followed by the PL ($\mu = -5.24, SD = .55$) segment and the DOWN segments ($\mu = -3.92, SD = .69$), all differences significant (PL, DOWN: $Z = -2.53, p = .01$; UP, DOWN: $Z = -2.53, p = .01$; UP, PL: $Z = -2.11, p = .03$). The vertical avoidance initiation time was lower in DVE than GVE, a difference that did not reach significance (GVE: $\mu = -5.52, SE = .26$; DVE: $\mu = -4.94, SE = .25$; GVE, DVE: $Z = 1.78, p = .07$). Of greater interest is the fact that pull-up was initiated one second earlier when gravitoinertial cues were present, a difference that was statistically significant (Cabin Motion ON: $\mu = -5.76, SD = 1.44$; Cabin Motion OFF: $\mu = -4.70, SD = 1.17$; ON, OFF: $Z = 1.99, p = .04$).

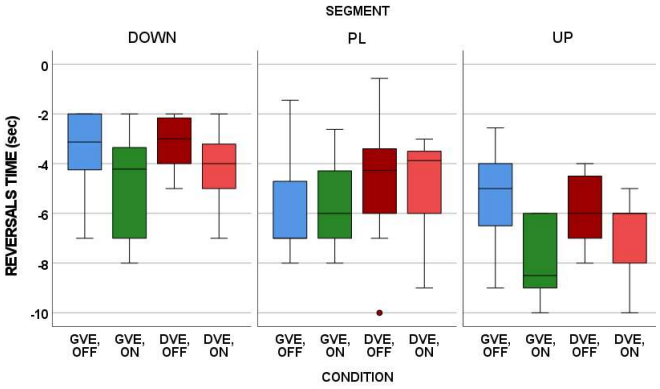

Figure 13: Boxplots of Reversals Time (sec) for the three Terrain segments, the two visibility levels, and the two gravitoinertial conditions.

These results do not necessarily relate to the presence of an obstacle, they can just be associated to the terrain. Therefore, need to investigate further with clear Max Time and Val.

Clearance at the start of the segments.

The effect of time of pull-up maneuver initiation is also observable in the clearance magnitude at the start of the segment. One can see that the clerance magnitude was significantly higher when an obstacle was present within the segment then without (Repeated-Measures ANOVA, Segment, Motion and Visibility as between subject variables: C0: $\mu = 14.38, SE = 1.41$; C1: $\mu = 22.87, SE = 1.80$; $F_{1,125} = 19.68, p < .0001$). There was also a significant effect of segment ($F_{2,125} = 110.54, p < .0001$; DOWN: PL: $t = -29.33, p < .0001$; DOWN, UP: $t = -50.26, p <$

.0001 ; PL,UP: $t = -20.93, p < .0001$). The clearance magnitude for DOWN segments was negative, both for C0 and C1, and not higher for C1 than C0 (C0, C1: $t = -6.02, p = .04$) indicating that obstacles were not likely detected before the descent. For PL and UP segments, conversely, the clearance magnitude was higher when an obstacle was present than not (PL: C0, C1: $t = -7.32, p = .01$; UP: C0, C1: $t = -12.02, p = .004$), suggesting that obstacles were detected before the segment, at least on some occurences. Note that magnitude of the difference between C0 and C1 was almost double for Up than PL segments.

Table 3: Clearance magnitude (ft, mean, SE) at the start of the DOWN, PL and UP segments for C0 and C1.

		DOWN	PL	UP
C0	Start	-10.88 (2.60)	17.61 (2.11)	36.35 (2.60)
C1	Start	-4.99 (3.31)	25.24 (2.69)	48.37 (3.31)

The effect of Visibility was significant and Clearance was overall higher by 7.3 ft in DVE than in GVE (GVE: $\mu = 14.93, SE = 1.87$, DVE: $\mu = 22.39, SE = 1.82$, GVE,DVE: $t = -7.39, p = .005$). There was no effect of interaction between Visibility and Segment. The effect of Motion was not significant.

Clearance at the locus of the Powerline Obstacle

Terrain Driven Clearance Profile

Determining the difference in altitude arising from the avoidance maneuver (climbing to fly above the obstacle and resume altitude before the obstacle) requires accounting for the position of the obstacle within a given segment to control for the flight envelope inherent to the terrain profile. One can see from the example in Figure x, that during descent (DOWN) and plateau (PL), clearance exceeded, at least in the vicinity of the Powerline obstacle, that of the exact same locus when no obstacle was present. Conversely, for the example of a UP segment, where the obstacle is located at the beginning of the descent, there is no difference in altitude between C0, C1 and C2 for the same position in the segment, because the pilot does not need additional clearance. Therefore, the position of the PWL in the segment will factor into the clearance behavior. Also, for this reason, computing averages over the entire segment will potentially not reflect the true estimates. To circumvent this issue, the following analyses will be using the estimates for the same position in space/time for the C0 and C1 cycles.

Comparing Performance within the Segment for C0 and C1

The following analyses will examine the effects of Segment on Clearance Magnitude difference and Climb Rate difference between C0 and C1. The powerline was "cleared" in 98.5% of the cases. Further analyses were performed on this sample set.

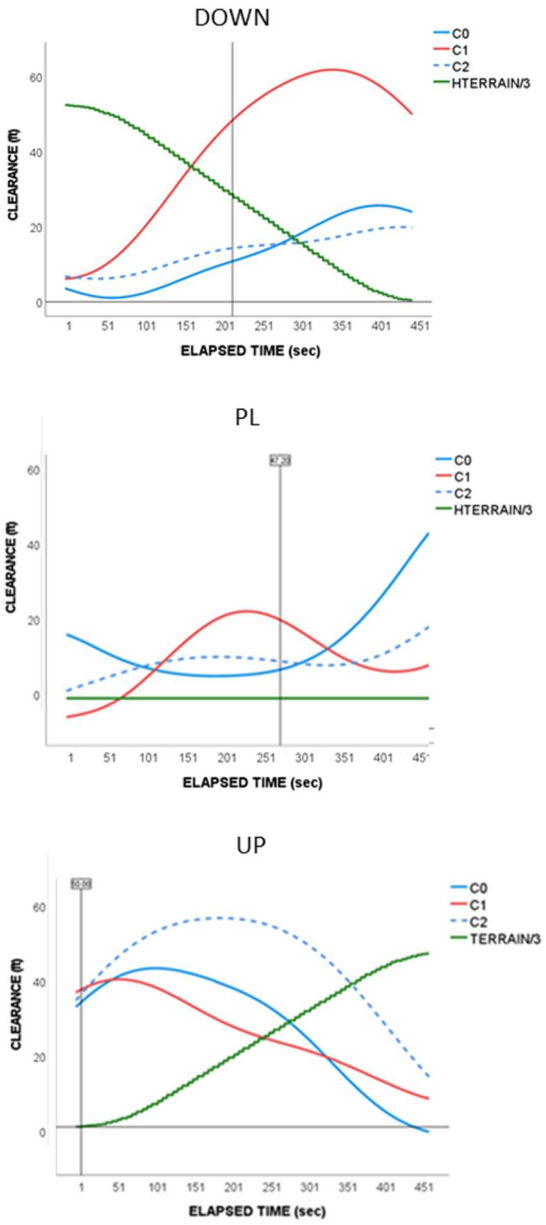

Figure 14: Clearance magnitude (ft above obstacle height, i.e., 55 ft) in the GVE, Cabin Motion OFF condition for Pilot P2, from left to right, for a DOWN, PL and UP segments, and the three Segment Cycles, C0, C1 and C2. Terrain profile for reference, altitude/3.

Note that the clearance at the locus of the obstacle is not the maximum clearance within the segment. The relative position of the maximum clearance in relation to the powerline position will be used later to discuss separately clearance maneuver initiation.

Figure 14 plots the Clearance magnitude (ft) and the Rate of Climb (ft/sec) at the locus of the powerline obstacle (C1) and the corresponding clearance magnitude and rate of climb for the same segment without obstacle (preceding cycle). Figure 15 plots the difference in Clearance magnitude and Rate of climb between C1 and C0.

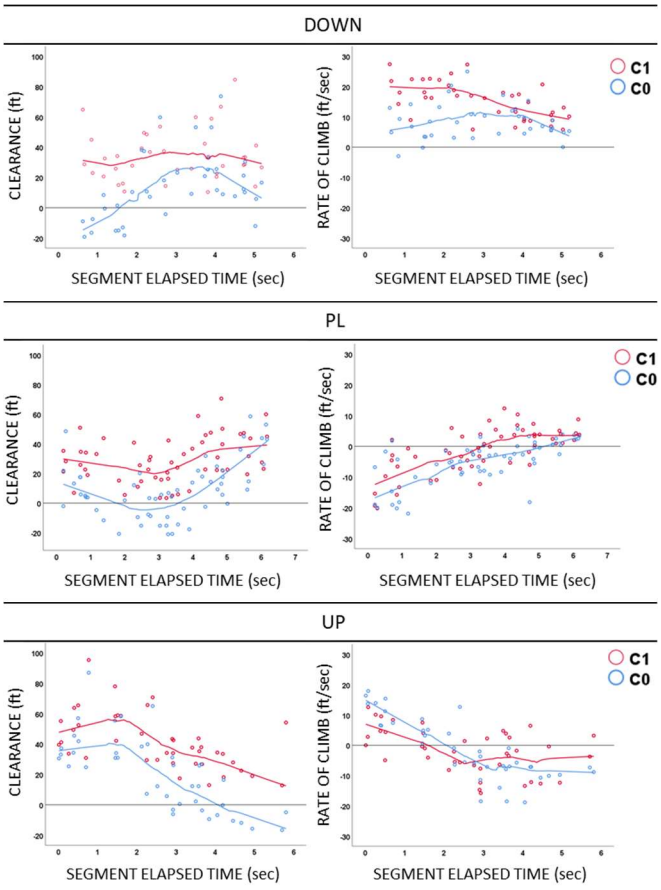

Figure 15: Clearance magnitude and Rate of Climb distributions as a function of the obstacle time for from top to bottom, DOWN, PL and UP segments. C0: No obstacle; C1: With Powerline Obstacle.

Because there is no strong assumption here regarding the relation between the dependent (clearance magnitude) and independent (segment elapsed time) variables, the distributions are fitted by LOESS line (using iterative weighted least squares for 50% of the data point) with an epanechnikov kernel function (data near the current point receive higher weights than extreme data receive).

One can see different patterns of differences as a function of the segment type. Clearance magnitude and Rate of Climb were *qualitatively and quantitatively different between segments and within segments.* For the DOWN segments, the clearance magnitude difference between C1 and C0 was maximum for obstacles located in the early part of the segment, i.e., at the beginning of the descent and reached a minimum for obstacles located close to the end of the descent. The opposite pattern was observed for UP segments, the clearance magnitude difference between C1 and C0 was minimum for obstacles located at the beginning of the segment, i.e., at the bottom of the hill and maximum for obstacles located at the end of the ascent. For PL segments, the maximum clearance magnitude difference was observed for obstacles located in the middle of the segment. Segments duration for each trial was discretized into three bins (Bin 1: .01 sec to 2.4 sec; Bin 2: 1.64 sec to 4.72 sec, Bin 3: 3.03 sec to 6.17 sec) to account for the observed major differences in clearance and rate of climb behavior. Repeated-measures ANOVA were performed to assess the effects of Segment type and Obstacle position within the segment on Clearance magnitude and univariate ANOVAS to quantify the effects of obstacle locus within the segment on the magnitude of the clearance difference as a function of the segment type.

Clearance magnitude was statistically higher for Cycle C1 (obstacle present) than for Cycle C0 (obstacle absent) (C0: $\mu = 13.38, SE = 1.53$; C1: $\mu = 34.72, SE = 1.36$; $F_{1,126} = 238.24, p < .0001$). The effect of Segment type was significant ($F_{2,126} = 4.79, p = .01$) and was significantly higher for the UP segment than for either the PL and DOWN segments. The effect of interaction between Cycle and Segment was not significant (DOWN: $\mu = 22.23, SE = 2.43$; PL: $\mu = 20.50, SE = 1.94$; UP: $\mu = 29.41, SE = 2.23$; PL, UP: $t = -8.90, p = .01$).

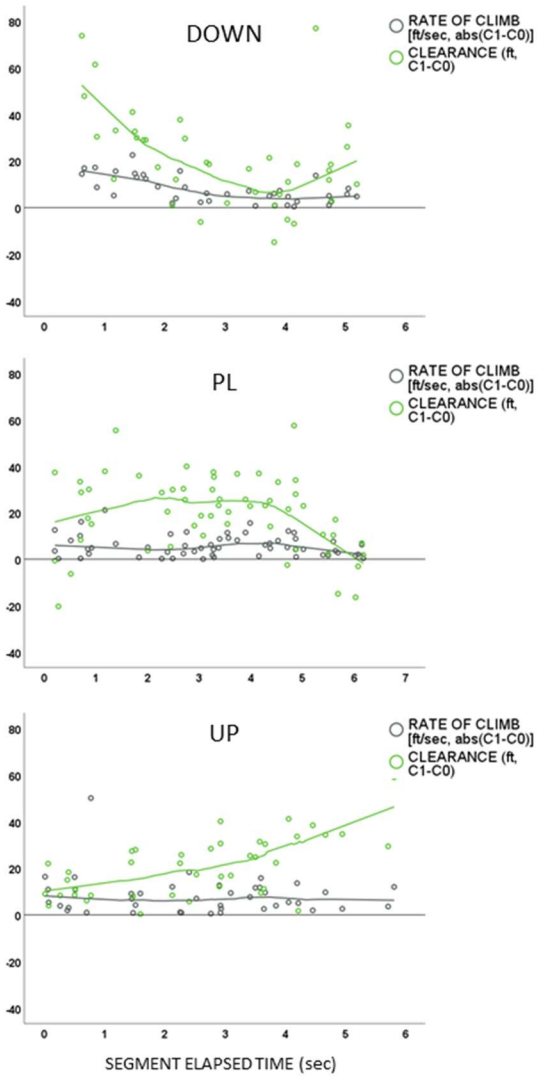

Figure 16: Clearance magnitude and Rate of Climb differences between C1 and C0 for from Top to Bottom, DOWN, PL and UP segments.

The effect of Bin was not significant ($F_{2,126} = 1.11, p = .33$), but the effects of interaction between Segment Type and Bin, and Cycle, Segment Type and Bin were highly significant (Segment Type * Bin: $F_{4,126} = 17.29, < .0001$; Cycle * Segment Type * Bin: $F_{4,126} = 7.24, p < .0001$).

For DOWN segments, Clearance magnitude difference between C0 and C1 significantly varied as a function of the position of the obstacle in the segment (Univariate ANOVA: Bin 1: $\mu = 39.16, SE = 5.67$; Bin 2: $\mu = 17.63, SE = 5.98$; Bin 3: $\mu = 13.35, SE = 4.11$; $F_{2,35} = 6.99, p = .003$) and was significantly higher for obtacles located at the beginning of the segment (Bin 1) than for obstacles located in the middle (Bin 2) or at the end of the segment (Bin 3) (Bin 1, Bin 2: $t = 21.52, p = .01$; Bin 2, Bin 3: $t = 4.28, p = .5$).

For Up segments, Clearance magnitude difference between C0 and C1 also significantly varied as a function of the position of the obstacle in the segment, but in a way opposote to that for the DOWN segments (Univariate ANOVA: $F_{2,38} = 8.63, p = .001$). Here, the highest clearance magnitude difference between C1 and C0 was observed for the obstacles located in the second and last parts of the segment (Bin 1: $\mu = 12.63, SE = 2.73$; Bin 2: $\mu = 22.14, SE = 3.03$; Bin 3: $\mu = 29.81, SE = 3.15$; Bin 1, Bin 2: $t = -9.51., p = .02$; Bin 2, Bin 3: $t = -7.67, p = .08$).

For PL segments, there was no statistical difference in clerance magnitude as a function of the locus of the powerline in the segment.

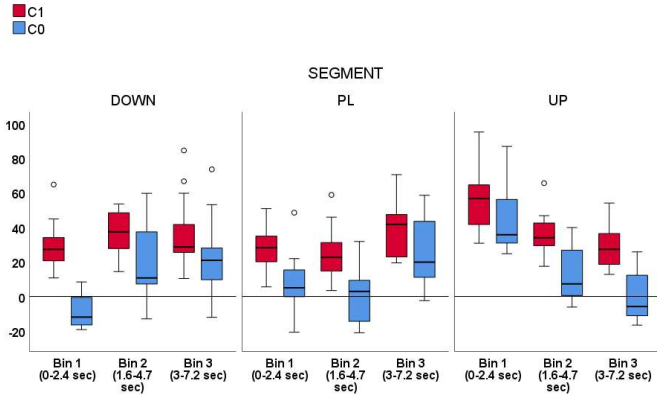

Figure 17: Clearance Magnitude (ft) for C0 and C1 as a function of the Obstacle position in the segment. From left to right: DOWN, PL and UP segments.

These results suggest that the variations in clearance magnitude between C0 and C1 attributable to the presence of an obstacle were dependent upon the type of segment and the position of the obstacle within the segment. When the nominal radar altitude associated with the terrain profile was low, like at the beginning of the descent or the end of an ascent, the pilots had to invcrease altitude to clear the obstacle. Conversely, when the radar altitude was already high, and sufficient to clear the obstacle, the added clearance associated to the presence of an obstacle was negligible.

Effects of Visibility and Motion on Clearance magnitude difference

For the DOWN segment, the magnitude of the clearance difference between C1 and C0 was higher in DVE than in GVE (NS) and Higher when Gravitoinertial cues were available (NS). There was a significant effect of interaction between Bin and Visibility ($F_{2,26} = 3.38, p = .04$). The highest difference in magnitude was observed in the DVE, ON condition in Bin 1, with a gain of 33ft when compared to the DVE, OFF condition. There was no facilitating effect of Motion in GVE.

For PL segments, one can see from Figure x that there was a consistent and significant effect of Motion (OFF: $\mu = 15.44, SE = 3.05$; ON: $\mu = 27.60, SE = 4.46$; OFF, ON: $t = -12.15., p = .03$) higher in DVE than GVE, with the highest Motion gain for Bins 1 and 2.

For UP segments, there was no evidence for effect of Motion or Visibility.

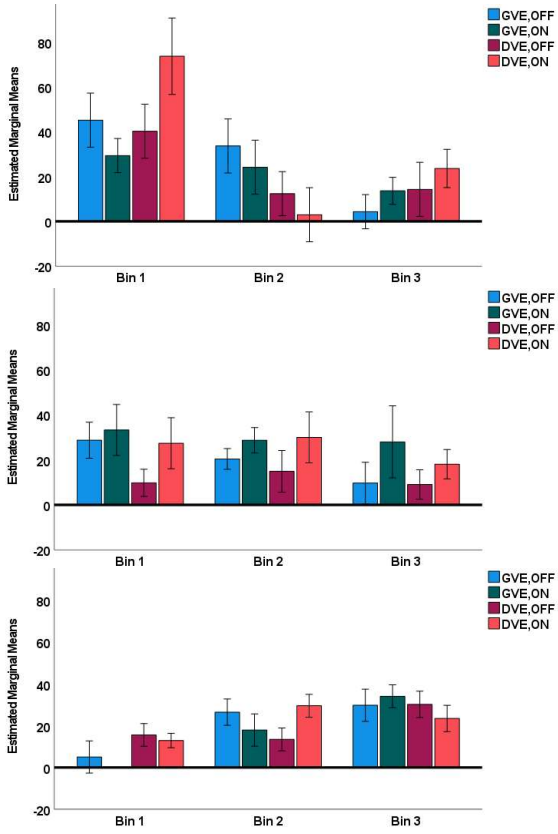

Figure 18: Clearance magnitude difference between C1 and C0 for from top to bottom, DOWN, PL and UP segments as a function of Visibility (GVE, DVE) and Motion (Cabin Motion ON, Cabin Motion OFF).

The Concept of Maximum Clearance and the Spatio-Temporal Proximity Window

Because it was observed that, in some instances, the nominal radar altitude requested by the terrain profile was sufficient to clear the powerline without or a very little additional climb, it

is obvious that the maximum clearance and the clearance at the locus of the obstacle were not always spatially and temporally coincident. If the pull-up maneuver is strictly guided by the obstacle, one may expect that the obstacle clearance and the maximum clearance to be close in time and space. Conversely, if the terrain guides primarily the current altitude, above the obstacle height, then some amount of separation in time and magnitude is expected between the maximum clearance and obstacle clearance. Figure 19 depicts the temporal relationships between Obstacle clearance and Max Clearance as a function of the locus of the powerline the segment. A +/-1 sec "Temporal Proximity" window represents the hypothetical limits for a true effect of Obstacle on Clearance Behavior. Figure 20 depicts the spatial relationships between Obstacle clearance and Max Clearance as a function of the locus of the powerline the segment. A 10ft "Spatial Proximity" window represents the hypothetical limits for a true effect of Obstacle on Clearance Behavior.

For DOWN segments, the highest Spatio-temporal contiguity is observed for obstacles located at the end of the segment, when normal radar altitude error is the lowest. The highest temporal discrepancy is observed at the beginning of the segment, where the Max clearance occurs up to 4 sec after the locus of the Obstacle (A positive value is associated to Maximum Clearance occurring after the obstacle).

For UP segments, we observe the opposite pattern, the highest Spatio-temporal contiguity is seen at the beginning of the ascent, when the radar altitude error is the highest. This result suggests that the obstacle was detected and reacted to before the segment started. The highest temporal discrepancy is observed at the end of the segment, where the Max clearance occurs up to 4 sec before the locus of the Obstacle (A negative value is associated to Maximum Clearance occurring before the obstacle).

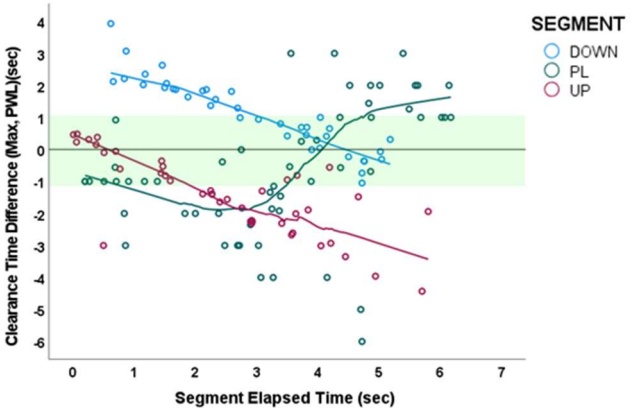

Figure 19: Time Difference between Powerline Obstacle Clearance and Maximum Clearance as a function of the position of the obstacle in the Segment. A Positive value is associated to Maximum Clearance occurring after the obstacle, a negative value refers to a Maximum Clearance occurring prior to the obstacle. A +/- 1 sec "Temporal Proximity" window represents the hypothetical limits for a true effect of Obstacle on Clearance Behavior.

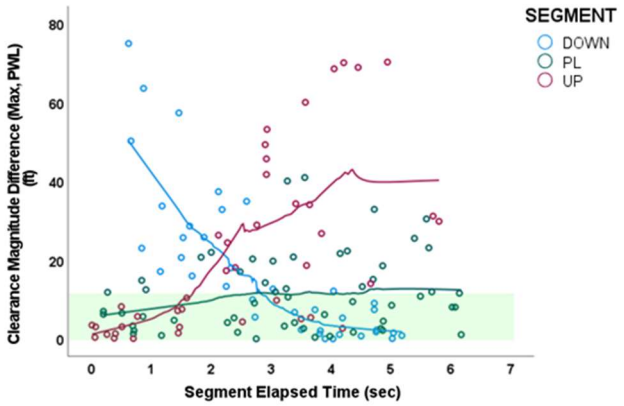

Figure 20: Clearance Magnitude Difference between Powerline Obstacle Clearance and Maximum Clearance as a function of the position of the obstacle in the Segment. A 10 ft "Spatial Proximity" window represents the hypothetical limits for a true effect of Obstacle on Clearance Behavior.

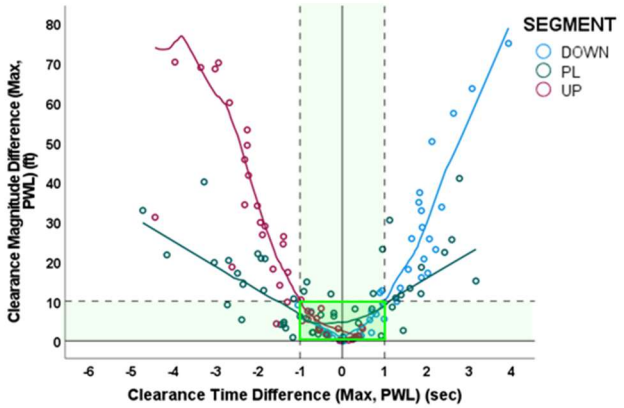

Figure 21: Magnitude difference between Max Clearance and Obstacle Clearance as a function of Time difference between Max Clearance and Obstacle Clearance. A Positive value for Clearance Time difference is associated to Maximum Clearance occurring after the obstacle, a negative value refers to a Maximum Clearance occurring prior to the obstacle. The green box at the intersection of the "Temporal Proximity" window and the "Spatial Proximity" window defines the probable region where the Pull-up maneuver was Obstacle-related.

For UP segments, we observe the opposite pattern, the highest Spatio-temporal contiguity is seen at the beginning of the ascent, when the radar altitude error is the highest. This result suggests that the obstacle was detected and reacted to before the segment started.

The highest temporal discrepancy is observed at the end of the segment, where the Max clearance occurs up to 4 sec before the locus of the Obstacle (A negative value is associated to Maximum Clearance occurring before the obstacle).

For PL segments, it is also observed both at the beginning and at the end of the segment, which is congruent with the data for

descent (the beginning of PL is the end of DOWN) and ascent (the end of PL is the beginning of UP). As one would expect, the difference in magnitude between Max clearance and Obstacle clearance is strongly associated to their temporal separation, as seen in Figure x. For DOWN and UP segments, more so for DOWN and UP segments.

The time difference between Max clearance and Obstacle clearance was used to create two categories: a "Proximal" category where the time difference is <=1 sec, and a "Distal" category for time differences >1 sec. This categorization was used to estimate the effects of Visibility and Motion on the Spatio-Temporal contiguity between Max Clearance and Obstacle Clearance.

Frequency of "Proximal" vs. "Distal" Cases

One can see from Table 4 that the percentage of "Proximal" represented on average half the cases, the highest percentage being observed for DOWN segments, and the lowest for UP segments (differences not statistically significant). The percentage of "Proximal" cases was overall higher in DVE (50%) than in GVE (41.8%) (NS) and lower without Motion (42%) than with Motion (50%).

In GVE, the percentage of "Proximal" cases is almost double for the DOWN than for the UP segment ($x_1^2 = 3.32, p = .06$). In DVE, there was no significant difference in the percentage of "Proximal" cases between the different segments. More interestingly is the fact that, for DOWN and UP segments, the percentage of "Proximal" cases is twice as high when Cabin Motion was ON (62.5%) than OFF (37.5%) ($x_1^2 = 3.5, p = .06$). This result is in line with the Sensory Weighted Approach of perception, which proposes that each sensory cue is weighted depending on this reliability. Typically, gravitoinertial information is attenuated when the visual information is of high relevance while it enhances performance when the visual information is less appropriate to perform the task (Modality Appropriateness Hypothesis, see Refs. 54, 55).

Table 4: Percentage of Spatio-Temporally "Proximal" cases as a function of the Segment Type, Visibility and Motion.

	DOWN	PL	UP
GVE, OFF	55.6%	36.8%	28,6%
GVE, ON	53.3%	45.5%	16.7%
GVE Total	54.2%	40%	23.1%
DVE, OFF	28.6%	56.3%	36.4%
DVE, ON	57.1%	40%	64.7%
DVE Total	42.9%	50%	53%
Total	50%	44.6%	43.9%

Table x: Magnitude difference between Max Clearance and Obstacle Clearance for "Proximal" category as a function of the Segment Type, Visibility and Motion.

	DOWN	PL	UP
GVE, OFF	4.87 (5.65)	2.42 (2.97)	1.56 (9.94)
GVE, ON	3.40 (4.47)	.95 (3.51)	5.05 (14.06)
DVE, OFF	6.11 (8.94)	8.23 (2.62)	3.54 (7.03)
DVE, ON	1.77 (6.32)	6.70 (3.93)	3.71 (4.24)

The examination of the magnitude of the differences between Max Clearance and Obstacle clearance shows a similar trend. For the "Proximal" category, Max Clearance and Obstacle Clearance difference was lower in GVE than DVE (GVE: $\mu = 2.91, SE = .70$; DVE: $\mu = 5.31, SE = .64$; GVE, DVE: $t = -2.40., p = .01$). Max Clearance and Obstacle Clearance difference was also lower with Cabin Motion ON than with Cabin Motion OFF, although the difference did not reach significance (OFF: $\mu = 4.93, SE = .68$; ON: $\mu = 3.29, SE = .65$; OFF, ON: $t = 1.64., p = .08$). However, there was a differential effect of Motion as a function of Visibility. In GVE, there was no effect of Motion cues on the magnitude of the clearance difference between Max and Obstacle (OFF: $\mu = 3.17, SE = .90$; ON: $\mu = 2.64, SE = .90$; OFF, ON: $t = .53., p = .68$). In DVE, conversely, the difference between Max and Obstacle clearance magnitude was significantly lower when Gravitoinertial cues were available (OFF: $\mu = 6.70, SE = 1.02$; ON: $\mu = 3.93, SE = .90$; OFF, ON: $t = 2.76., p = .05$) and the magnitude of the differences between Max Clearance and Obstacle Clearance was not statistically different than that in GVE when Motion cues were available. Last, spatial proximity was achieved to a greater extent for the Down segments, and to some degree for the PL segments.

CONCLUSIONS

The aim of this experiment was to assess the contributions of gravitoinertial and visual cues in two conditions, to evaluate 1. the relative contribution of Visual and Gravitoinertial cues in the perception of altitude in low-level forward flight and 2. How the Sense of Agency may interact with the perception and integration mechanisms. In the first condition, referred to as Supervisory Control condition, pilots were asked to passively report their perceived altitude above the ground level (AGL) while moving in a simulated NOE flight in AP mode. In the second condition, referred to as Active Control condition, the pilots had to actively regulate their altitude, speed and heading as if they were in a real NOE situation. The two conditions requiring different perception mechanisms. In the Supervisory Control Task, the representation of the self in the environment relies on the integration of relative cues during visual *perception decoupled from action*, where the pilot is experiencing a reduced Sense of Agency. Conversely, in the Active Control Task, the representation of the self in the environment is mediated by *control-oriented action-*

perception mechanisms, where the pilot has a strong sense of control.

The results for the Supervisory Control task showed that the gravitoinertial component played a significant role in the estimation of ground height, but only in the case where the optical structure did not specify efficiently the actor-environment interaction. The improvement of the tracking performance in the visuo-vestibular setting as compared to a visual only setting when the visual cues were poor indicated some level of multisensory integration.

Similarly, the results for the Active Control task provided evidence, at multiple levels, that the acceleration information, specified by the variations of the gravitoinertial field, has a relative character.

First, Pull-Up Initiation Time was facilitated by the presence of gravitoinertial cues, leading to a gain of 1 sec in DVE. Second, the magnitude of the clearance difference between C1 and C0 was higher in DVE than in GVE and higher when Gravitoinertial cues were available. The highest difference in magnitude between C0 and C1 was observed for DOWN segments with a gain of 33ft with Motion cues when compared to the DVE, OFF condition.

Thirdly, and of most importance, is the result that 1. "Spatio-Temporal" proximity between Maximum Clearance and Obstacle Clearance was lowere in DVE than in GVE, but that 2. Motion cues mitigated the deleterious effects of DVE, and that the presence of motion cues led to equivalent performance than in GVE.

Altogether, these results is in line with the Sensory Weighted Approach of perception, which proposes that each sensory cue is weighted depending on this reliability. Typically, gravitoinertial information is attenuated when the visual information is of high relevance while it enhances performance when the visual information is less appropriate to perform the task (Modality Appropriateness Hypothesis, see Refs. 54, 55). According to the Bayesian probability theory (Refs. 6, 49, 50, 51), the relative unisensory weights depend on specific integration patterns. The experimental conditions tested in this simulation prevented the testing of the Maximum Likelihood Estimate model, because the purely gravitoinertial condition (no visual cues) was not provided.

One of the main difficulties in the Active Control task was to differentiate the effects of terrain from the "true" effects of the powerline obstacle. Clearance magnitude and Rate of Climb were *qualitatively and quantitatively different between segments and within segments*, which creates ambiguity regarding the origin of the differences in performance between the nominal and off-nominal cycles in a trial. Inded the variations in clearance magnitude between C0 and C1 attributable to the presence of an obstacle were dependent upon the type of segment and the position of the obstacle within the segment. When the nominal radar altitude associated with the terrain profile was low, like at the beginning of the descent or the end of an ascent, the pilots had to invcrease altitude to clear the obstacle. Conversely, when the radar altitude was already high, and sufficient to clear the obstacle, the added clearance associated to the presence of an obstacle was negligible. Further research will investigate how pull-up control strategy (cyclic and collective) and tau theory could be used to account for the perfromance data in both the Supervisory and Control Task.

Author contact: Martine Godfroy-Cooper
martine.godfroy@sjsu.edu.

REFERENCES

1. Gibson, J. J., "The Perception of Visual Surfaces," *The American Journal of Psychology*, 1950; 63, No.3, pp. 367-384.
2. Berthier, N. E., Clifton, R. K., Gullapalli, V., McCall, D., Robin, D. J., "Visual Information and Object Size in the Control of Reaching," *Journal of Motor Behaviour*, 1996; 28, No. 3, pp. 187-197.
3. Jürgens, R., Becker, W., "Human spatial orientation in non-stationary environments: relation between self-turning perception and detection of surround motion," *Exp Brain Res*, 2011; 215, pp. 327-344.
4. Stoffregen, T. A., Riccio, G. E., "An ecological theory of orientation and the vestibular system," *Psychological review*, 1988; 95(1), pp. 3-14.
5. Wright, G. W., DiZio, P., Lackner, R. J., "Vertical linear self-motion perception during visual and inertial motion: More than weighted summation of sensory inputs," *Journal of Vestibular Research*, 2005; 15, No.4, pp. 185-195.
6. Fetsch, C. R., Turner, A. H., DeAngelis, G. C., Angelaki, D. E., "Dynamic reweighting of visual and Vestibular Cues during Self-Motion Perception," *Journal of Neuroscience*, 2009; No. 49, pp. 15601-15612.
7. Sekuler, R., Watamaniuk, S. N., Blake, R., Yantis, S., Pashler, H., "Stevens's handbook of experimental psychology", *Sensation and Perception*, 2002; 1:121-53.
8. St George, R.J., Day, B.L. and Fitzpatrick, R.C., Adaptation of vestibular signals for self-motion perception, *The Journal of physiology*, 2011, 589(4), pp.843-853.
9. Antunano, M. J., & Mohler, S. R., "Inflight spatial disorientation", *Human Factors & Aviation Medicine*, 1992, 39(1).
10. Johnson, W.W., Schroeder, J. and Statler, I.C., "Visual-Motion Cueing in Altitude and Yaw Control", 1994.
11. Abdur-Rahim, J., Collet, A.C., Le Goff, K., Rakotomamonjy, T., Juppet, V., Moreau, S. J., Descatoire, T., Landrieu, J., Plat-Robain, M., Denquin, F., Sarrazin, J.C., & Bardy, B. (submitted), "Lost in rotation, not so in translation: Infraliminary and supraliminary thresholds detection for detecting rotational and /translational stimulation motion using a whole-body VR motion simulator".

12. Péruch, P., & Wilson, P.N., "Active versus passive learning and testing in a complex outside built environment", *Cognitive Processing,* 5, 2004, 218–227.

13. Haggard, P., & Tsakiris, M., "The Experience of Agency: Feelings, Judgments, and Responsibility", *Current Directions in Psychological Science,* 18(4), 2009, 242-246.

14. Haggard, P., "Sense of agency in the human brain.", *Nature Review Neuroscience,* 18(4), 2017, pp. 196-207.

15. Berberian, B., Sarrazin, J. C., Le Blaye, P., & Haggard, P. (2012). "Automation technology and sense of control: a window on human agency". *PLoS One*, *7*(3), e34075.

16. Runeson S. *On visual perception of dynamic events*. Acta Universitatis Upsaliensis; 1983.

17. Fajen, R. B., "The scaling of information to action in visually guided braking", *Journal of experimental psychology: human perception and performance.* 2005; 31, No. 5, p.1107.

18. Brenner, E., Van Den Berg, A. V., Van Damme, W. J., "Perceived motion in depth", *Vision Research*, 1996; 36, No. 5, pp. 699-706.

19. Warren, W. H., Young, D. S., Lee, D. N., "Visual Control of Step Length During Running Over Irregular Terrain," *Journal of experimental psychology: human perception and performance.* 1986;12, No. 3, pp. 259-266

20. Mantel, B., Stoffregen, T. A., Campbell, A., Bardy, B. G., "Exploratory movement generates higher-order information that is sufficient for accurate perception of scaled egocentric distance," *PloS One*. 2015;10, No. 4.

21. Flach, J. M., Warren, R., Garness, S. A., Kelly, L., & Stanard, T., "Perception and control of altitude: Splay and depression angles," *Journal of Experimental Psychology: Human Perception and Performance*, 23(6), 1997, 1764.

22. Owen, D. H., & Warren, R., "Perceptually relevant metrics for the margin of safety: A consideration of global optical flow and density variables," *Ohio State Univ. Res. Foundation, Columbus, OH,*1982.

23. Warren, W. H., Morris, M. W., & Kalish, M., "Perception of translational heading from optical flow," *Journal of Experimental Psychology: Human Perception and Performance*, 14(4), 1988, 646.

24. Biggs, N. L., "Directional guidance of motor vehicles: A preliminary survey and analysis," *Ergonomics,* 9, 1966, 193-202.

25. Lee, D. N., "A theory of visual control of braking based on information about time to collision," *Perception*, 5, 1976, 437-459.

26. Lee, D. N., "The optic flow field: The foundation of vision," Philosophical Transactions of the Royal Society of London, Series B, 290, 1980, 169-179.

27. Denton, G. G., "The influence of visual pattern on perceived speed," *Perception*, *9*(4), 1980, 393-402.

28. Kleiss, J. A., & Hubbard, D. C., "Effects of three types of flight simulator visual scene detail on detection of altitude change," *Human factors*, *35*(4), 1993, 653-671.

29. Sedgwick, H. A., "Space perception," *Sensory process and perception*, 1986.

30. Patterson, R., Geri, G. A., Dyre, B. P., Akhtar, S. C., Covas, C. M. and Pierce, B. J., "Altitude control in simulated flight using 3-D objects and terrain texture," *Journal of the Society for Information Display*, *13*(12), 2005, pp.1039-1043.

31. Leung, T., & Malik, J., "On perpendicular texture or: Why do we see more flowers in the distance?" *Proceedings of IEEE Computer Society Conference on Computer Vision and Pattern Recognition* (pp. 807-813), IEEE, 1997.

32. Gray, R., Geri, G. A., Akhtar, S. C., & Covas, C. M., "The role of visual occlusion in altitude maintenance during simulated flight," *Journal of Experimental Psychology: Human perception and performance*, *34*(2), 2008, 475.

33. Goodale, M. A., Milner, D. A., Separate visual pathways for perception and action. 1992.

34. Hu Y., Goodale, M. A., "Grasping after a delay shifts size-scaling from absolute to relative metrics," *Journal of Cognitive Neuroscience*. 2000;12, No. 5, pp. 856-868.

35. Knol, H. Aiming for illusions: The perception of size and its influence on motor control. Doctoral dissertation. 2016.

36. Ungs, T. J., "The occurrence of the vection illusion among helicopter pilots while flying over water," *Aviation, space, and environmental medicine*. 1989; 60, No. 11, pp. 1099-1101.

37. Newman, D. G., FAICD A. An overview of spatial disorientation as a factor in aviation accidents and incidents. 2007; No. B2007/0063, p. 14.

38. Tredici, T. J., "Visual illusions as a probable cause of aircrafts accidents," S*patial Disorientation in Flight: Current Problems*. 1980; pp. 1-5.

39. Riccio, G. E., Martin, E. J., Stoffregen, T. A., "The role of balance dynamics in the active perception of orientation," *Journal of Experimental Psychology:*

Human Perception and Performance. 1992;18, No. 3, p. 624.

40. Török, A., Ferrè, E. R., Kokkinara, E., Csépe, V., Swapp, D., Haggard, P., "Up, down, near, far: an online vestibular contribution to distance judgement," *PloS One*. 2017;12, No. 1.
41. Benson, A. J., "Sensory functions and limitations of the vestibular system", in *The Perception and Control of Self-motion*, Eds R. Warren, A. H. Wertheim (Hillsdale, NJ: Lawrence Erlbaum Associates), 1990, pp 154–157.
42. Angelaki, D. E., Cullen, K. E., "Vestibular system: the many facets of a multimodal sense," *Annu. Rev. Neurosci*. 2008;31, pp. 125-150.
43. Lopez, C., & Blanke, O., "The thalamocortical vestibular system in animals and humans," *Brain research reviews*, *67*(1-2), 2011, 119-146.
44. Fetsch, C. R., DeAngelis, G. C., Angelaki, D. E., "Visual-vestibular cue integration for heading perception: application of optimal cue integration theory," *European Journal of Neuroscience*. 2010; 31, No. 10, pp. 1721-1729.
45. De Winkel, K. N., Soyka, F., Barnett-Cowan, M., Bülthoff, H. H., Groen, E. L., Werkhoven, P. J., "Integration of visual and inertial cues in the perception of angular self-motion," *Experimental brain research*. 2013; 231, No. 2, pp. 209-218.
46. Gradwell, D., Rainford, D., *Ernsting's aviation medicine*. Hodder Education, 2006, 2006; pp. 451-453.
47. Pagels, A., Hagelen, M., Briese, G., Tessman, A., "Helicopter assisted landing system-millimeter-wave against brown-out," *German Microwave Conference*. IEEE. 2009; pp. 1-3.
48. Körding, K. P., Beierholm, U., Ma, W. J., Quartz, S., Tenenbaum, J. B., Shams, L., "Causal inference in multisensory perception," *PloS One*. 2007; 2, No. 9.
49. Jacobs A. R., "Optimal integration of texture and motion cues to depth," *Vision research*. 1999; 39, No. 21, pp. 3621-3629.
50. Ernst, O. M., Banks, M. S., "Human integrate visual and haptic information in a statistically optimal fashion," *Nature*. 2002; 415, No. 6870, pp. 429-433.
51. Butler, J. S., Smith, S. T., Campos, J. L., Bülthoff, H. H., "Bayesian integration of visual and vestibular signals for heading," *Journal of vision*. 2010; 10 No. 11, p. 23.
52. Stoffregen, T. A., Bardy, B. G., "On specifications and the senses," *Behavioral and Brain Sciences*. 2001; 24, No. 2, pp. 195-213.
53. DeAngelis, G. C., & Angelaki, D. E., "Visual–vestibular integration for self-motion perception," In *The neural bases of multisensory processes*. CRC Press/Taylor & Francis, 2012.
54. Welch, R. B., "Meaning, attention, and the "unity assumption" in the intersensory bias of spatial and temporal perceptions," In *Advances in psychology* (Vol. 129, pp. 371-387). North-Holland, 1999.
55. Godfroy-Cooper, M., Sandor, P. M. B., Miller, J. D., & Welch, R. B., "The interaction of vision and audition in two-dimensional space," *Frontiers in neuroscience*, *9*, 2015, 311.
56. Gibb, R., Ercoline, B., & Scharff, L., "Spatial disorientation: decades of pilot fatalities," *Aviation, space, and environmental medicine*, *82*(7), 2011, 717-724.
57. Endsley, M. R., & Kiris, E. O. (1995). The out-of-the-loop performance problem and level of control in automation. *Human factors*, *37*(2), 381-394.
58. Somon, B., Campagne, A., Delorme, A., & Berberian, B. (2017). Performance monitoring applied to system supervision. *Frontiers in human neuroscience*, *11*, 360.
59. Gouraud, J., Delorme, A., & Berberian, B. (2017). Autopilot, mind wandering, and the out of the loop performance problem. *Frontiers in neuroscience*, *11*, 541.
60. Skitka, L. J., Mosier, K. L., & Burdick, M. (1999). Does automation bias decision-making? *International Journal of Human-Computer Studies*, *51*(5), 991-1006.
61. Louw, T., & Merat, N. (2017). Are you in the loop? Using gaze dispersion to understand driver visual attention during vehicle automation. *Transportation Research Part C: Emerging Technologies*, *76*, 35-50.
62. De Vignemont, F., & Fourneret, P. (2004). The sense of agency: A philosophical and empirical review of the "Who" system. *Consciousness and Cognition*, *13*(1), 1-19.
63. Wegner, D. M., & Wheatley, T. (1999). Apparent mental causation: Sources of the experience of will. *American psychologist*, *54*(7), 480.
64. Coyle, D., Moore, J., Kristensson, P. O., Fletcher, P., & Blackwell, A. (2012, May). I did that! Measuring users' experience of agency in their own actions. In *Proceedings of the SIGCHI conference on human factors in computing systems* (pp. 2025-2034).